

Novel Lanthanide Coordination Polymers with a Flexible Disulfoxide Ligand, 1,2-Bis(ethylsulfinyl)ethane: Structures, Stereochemistry, and the Influences of Counteranions on the Framework Formations

Jian-Rong Li,[†] Xian-He Bu,^{*,†,‡} and Ruo-Hua Zhang[†]

Department of Chemistry, Nankai University, Tianjin 300071, China, and the State Key Laboratory of Rare Earth Materials Chemistry and Applications, Peking University, Beijing 100871, China

Received July 7, 2003

The reactions of *meso*-1,2-bis(ethylsulfinyl)ethane (*meso*-L) with Ln(ClO₄)₃ [Ln(NO₃)₃ or Ln(NCS)₃] in MeOH and CHCl₃ gave a series of new lanthanide coordination polymers, {[Ln(*μ*-*meso*-L)(*rac*-L)₂(CH₃OH)₂](ClO₄)₃]_n [Ln: La (1), Nd (2), Eu (3), Gd (4), Tb (5), Dy (6), and Yb (7)], [Yb(*μ*-*meso*-L)_{1.5}(NO₃)₃]_n (8), and [La(*μ*-*meso*-L)_{2.5}(NCS)₃]_n (9). All the structures were established by single-crystal X-ray diffraction. Complexes 1–7 are isostructural with infinite single *μ*-chain structure, in which the L ligands take two kinds of coordination modes: bidentate chelating and bis-monodentate bridging. Six sulfur atoms of the sulfoxide groups around each Ln^{III} center adopt alternatively the same *R* or *S* configuration in the chain. In addition, the configuration change of partial ligands occurred from the *meso* to the *rac* form when reacting with Ln(ClO₄)₃. To our knowledge, this is the first example of disulfoxide complexes with two kinds of coordination modes and three kinds of configurations (*R,R*, *S,S*, and *R,S*) occurring simultaneously in the same complex. 8 exhibits single–double bridging chain structure, in which dinuclear macrometallacycles formed through bridging two Yb^{III} by two *meso*-L ligands are further linked by another *meso*-L ligand. In 9 each La^{III} ion is linked to five other La^{III} ions by five *meso*-L ligands to form a 5-connected 2-D (3/4,5) network containing two types of macrometallacyclic arrays: quadrilateral and triangle grids. The structural differences among 1–7, 8, and 9 show that counteranions play important roles in the framework formation of such coordination polymers. In addition, the luminescent properties of 3 and 5 were also investigated.

Introduction

Coordination frameworks constructed by linking organic multifunctional ligands with metal ions are attracting great attention in current coordination chemistry due to their fascinating structural topologies and potential applications.¹ The majority of the reported work so far has been the complexes with polydentate rigid ligands,² while the use of flexible ligands as building blocks in the construction of coordination polymers has been comparatively less.³ However, such ligands are attractive because their flexibility and conformation freedoms may offer higher possibility for the construction of unique frameworks with useful properties.

The flexible disulfoxide ligands have many intriguing features, such as the bidentate ditopic nature, the inherent chiral

properties of the sulfur atom, and the diastereomeric *meso* and *rac* forms. They can coordinate to metal ions *via* either O or S donors according to their electronic and steric factors to form extended structures.^{4–8} In addition, the configuration inversion of the sulfur atoms in the disulfoxide molecules may take place when reacting with metal ions.⁹ As for

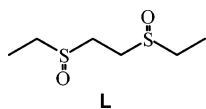
- (1) For recent reviews, see: (a) Evans, O. R.; Lin, W.-B. *Acc. Chem. Res.* **2002**, *35*, 511. (b) Gade, L. H. *Acc. Chem. Res.* **2002**, *35*, 575. (c) Seidel, S. R.; Stang, P. J. *Acc. Chem. Res.* **2002**, *35*, 972. (d) Moulton, B.; Zaworotko, M. J. *Chem. Rev.* **2001**, *101*, 1629. (e) Eddaoudi, M.; Moler, D. B.; Li, H.-L.; Chen, B.-L.; Reineke, T. M.; O'Keeffe, M.; Yaghi, O. M. *Acc. Chem. Res.* **2001**, *34*, 319. (f) Fujita, M.; Umamoto, K.; Yoshizawa, M.; Fujita, N.; Kusakawa, T.; Biradha, K. *Chem. Commun.* **2001**, 509. (g) Swiegers, G. F.; Malefetse, T. J. *Chem. Rev.* **2000**, *100*, 3483. (h) Braga, D. *J. Chem. Soc., Dalton Trans.* **2000**, 3705. (i) Robson, R. *J. Chem. Soc., Dalton Trans.* **2000**, 3735. (j) Piguet, C.; Bünzli, J.-C. G. *Chem. Soc. Rev.* **1999**, *28*, 347. (k) Blake, A. J.; Champness, N. R.; Hubberstey, P.; Li, W.-S.; Withersby, M. A.; Schröder, M. *Coord. Chem. Rev.* **1999**, *183*, 117. (l) Batten S. R.; Robson, R. *Angew. Chem., Int. Ed.* **1998**, *37*, 1461. (m) Zhao, H.; Bazile, M. J., Jr.; Galán-Mascarós, J. R.; Dunbar, K. R. *Angew. Chem., Int. Ed.* **2003**, *42*, 1015.

* Corresponding author. E-mail: buxh@nankai.edu.cn. Fax: +86-22-23502458.

[†] Nankai University.

[‡] Peking University.

Chart 1



lanthanide disulfoxide complexes, several polymers with chain or framework structures were reported by us and others.^{5d,8c-f} These results indicate that the construction of high dimensional lanthanide coordination polymers is possible by selecting suitable disulfoxide ligands as building blocks. As a continuation of our efforts to explore new structural types and special properties of lanthanide complexes with such ligands, we report herein the synthesis, structures, and stereochemical features of the lanthanide coordination polymers with a flexible disulfoxide ligand, 1,2-bis(ethylsulfinyl)ethane (**L**, Chart 1), {[Ln(μ -*meso*-**L**)(*rac*-**L**)₂(CH₃OH)₂](ClO₄)₃]_n [La (**1**), Nd (**2**), Eu (**3**), Gd (**4**), Tb (**5**), Dy (**6**), and Yb (**7**)], [Yb(μ -*meso*-**L**)_{1.5}(NO₃)₃]_n (**8**), and [La(μ -*meso*-**L**)_{2.5}(NCS)₃]_n (**9**). To our knowledge, the iso-

structural complexes **1–7** are the first examples of disulfoxide complexes with two kinds of coordination modes and three kinds of ligand configurations occurring simultaneously in the same complex. The luminescent properties of complexes **3** and **5** and the counteranion effects on the structures of the complexes with this type of disulfoxide ligand will also be discussed.

Experimental Section

Materials and General Methods. All reagents for syntheses and analyses were of analytical grade and purified by standard methods prior to use. Elemental analyses were carried out on a Perkin-Elmer 240C analyzer. Melting point measurements were taken on an X-4 melting point meter. ¹H NMR spectra were recorded on a Bruker AC-P500 spectrometer (300 MHz) at 25 °C with tetramethylsilane as the internal reference. IR spectra were measured on a 170SX (Nicolet) FT-IR spectrometer with KBr pellets. Thermal analyses were carried out on a NETZSCH TG 209 instrument. The solid-state excitation and emission spectra were obtained at room temperature on an Edinburgh Analytical Instruments FLS920 spectrofluorometer.

Synthesis of *meso*-1,2-Bis(ethylsulfinyl)ethane (*meso*-L**).** 1,2-Bis(ethylsulfinyl)ethane (**L**) was synthesized according to a similar literature method.¹⁰ The *meso* isomer of **L** (mp: 141–143 °C) was separated from the *rac* isomer (mp: 124–126 °C) by fractional crystallization from acetone. Yield: 45%. Single crystals of *meso*-**L** suitable for X-ray analysis were obtained by ether diffusing to its chloroform solution. Anal. Calcd for C₆H₁₄O₂S₂ (%): C, 39.56; H, 7.69. Found: C, 39.27; H, 7.25. ¹H NMR (CDCl₃): δ 1.38 (t, 6H, CH₃–), 2.83 (q, 4H, –CH₂S–), 2.98–3.22 (m, 4H, –S(CH₂)₂S–). IR (KBr pellet, cm⁻¹): 2962m, 1431m, 1384m, 1034m, 1018s, 770m, 681m.

Synthesis of {[Ln(μ -*meso*-L**)(*rac*-**L**)₂(CH₃OH)₂](ClO₄)₃]_n (**1–7**).** The complexes **1–7** were synthesized by the procedure described below: triethylorthoformate (4 mL) was added to an anhydrous methanol solution (6 mL) of Ln(ClO₄)₃·nH₂O (0.2 mmol), and the mixture was stirred for ca. 30 min. The ligand (*meso*-**L**, 0.6 mmol) in CHCl₃ (6 mL) was added dropwise to the above mixture, and after the mixture was stirred at 70–80 °C for 4 h, the white precipitate was collected and washed with several portions of anhydrous MeOH/CHCl₃ and ether, respectively, and dried in vacuo. The crystals were obtained by layered-diffusing an MeOH solution (4 mL) of Ln(ClO₄)₃·nH₂O (0.05 mmol) on a CHCl₃ solution (4 mL) of *meso*-**L** (0.15 mmol) using triethylorthoformate (3 mL) as a “buffer layer” and also dehydrating reagent.

WARNING! Although we experienced no problems in handling perchlorate compounds, these should be handled with great caution due to their potential for explosion.

{[La(μ -*meso*-**L**)(*rac*-**L**)₂(CH₃OH)₂](ClO₄)₃]_n (**1**). Yield: 58%. Anal. Calcd for C₂₀H₅₀Cl₃O₂₀S₆La (%): C, 22.92; H, 4.81. Found: C, 22.50; H, 4.31. IR (KBr pellet, cm⁻¹): 3405s, 1645m, 1457w, 1412w, 1146s, 1114s, 1087s, 1004s, 778w, 683m, 637m, 627s. Decomposition temperature: 198 °C.

{[Nd(μ -*meso*-**L**)(*rac*-**L**)₂(CH₃OH)₂](ClO₄)₃]_n (**2**). Yield: 54%. Anal. Calcd for C₂₀H₅₀Cl₃O₂₀S₆Nd (%): C, 22.80; H, 4.78. Found: C, 22.31; H, 4.25. IR (KBr pellet, cm⁻¹): 3385s, 1635m, 1458w, 1417w, 1147s, 1088s, 999s, 780w, 682w, 637m, 626m. Decomposition temperature: 201 °C.

(10) Zhang, R.-H.; Zhan, Y.-L.; Chen, J.-T. *Synth. React. Inorg. Met.-Org. Chem.* **1995**, *25*, 283.

- (2) For examples: (a) Chen, B.-L.; Eddaoudi, M.; Hyde, S. T.; O’Keeffe, M.; Yaghi, O. M. *Science* **2001**, *291*, 102. (b) Noro, S.-I.; Kitaura, R.; Kondo, M.; Kitagawa, S.; Ishii, T.; Matsuzaka, H.; Yamashita, M. *J. Am. Chem. Soc.* **2002**, *124*, 2568. (c) Cussen, E. J.; Claridge, J. B.; Rosseinsky, M. J.; Kepert, C. J. *J. Am. Chem. Soc.* **2002**, *124*, 9574. (d) Long, D.-L.; Blake, A. J.; Champness, N. R.; Wilson, C.; Schröder, M. *Chem. Eur. J.* **2002**, *8*, 2026. (e) Carlucci, L.; Ciani, G.; Proserpio, D. M.; Rizzatob, S. *New J. Chem.* **2003**, *27*, 483.
- (3) (a) Hennigar, T. L.; MacQuarrie, D. C.; Losier, P.; Rogers, R. D.; Zaworotko, M. J. *Angew. Chem., Int. Ed. Engl.* **1997**, *36*, 972. (b) Duncan, P. C. M.; Goodgame, D. M. L.; Menzer, S.; Williams, D. J. *Chem. Commun.* **1996**, 2127. (c) Carlucci, L.; Ciani, G.; Gudenberg, D. W.; Proserpio, D. W. *Inorg. Chem.* **1997**, *36*, 3812. (d) van Albada, G. A.; Guijt, R. C.; Haasnoot, J. G.; Lutz, M.; Spek, A. L.; Reedijk, J. *Eur. J. Inorg. Chem.* **2000**, 121. (e) Fei, B.-L.; Sun, W.-Y.; Okamura, T.; Tang, W.-X.; Ueyama, N. *New J. Chem.* **2001**, *25*, 210.
- (4) (a) Calligaris, M.; Melchior, A.; Geremia, S. *Inorg. Chim. Acta* **2001**, *323*, 89. (b) Geremia, S.; Calligaris, M.; Mestroni, S. *Inorg. Chim. Acta* **1999**, *292*, 144. (c) Calligaris, M.; Carugo, O. *Coord. Chem. Rev.* **1996**, *153*, 83.
- (5) (a) Ayala, J. D.; Bombieri, G.; Pra, A. D.; Fantoni, A.; Vicentini, G. *Inorg. Chim. Acta* **1998**, *274*, 122. (b) Ayala, J. D.; Bombieri, G.; Pra, A. D.; Vicentini, G. *Inorg. Chim. Acta* **1998**, *274*, 236. (c) Ayala, J. D.; Zinner, L. B.; Vicentini, G.; Pra, A. D.; Bombieri, G. *Inorg. Chim. Acta* **1993**, *211*, 161. (d) Miranda, J. M.; Oliveira, M. A.; Castellano, E. E.; Scoralick, E.; Zinner, L. B.; Vicentini, G. *Inorg. Chim. Acta* **1987**, *139*, 131.
- (6) (a) Sousa, G. F. De; Filgueiras, C. A. L.; Nixon, J. F.; Hitchcock, P. B. *J. Braz. Chem. Soc.* **1997**, *8*, 649. (b) Carvalho, C. C. C.; Francisco, R. H. P.; Gambardella, M. T. Do P.; Sousa, G. F. De; Filgueiras, C. A. L. *Acta Crystallogr., Sect. C* **1996**, *52*, 1629.
- (7) (a) Sacht, C.; Datt, M. S.; Otto, S.; Roodt, A. *J. Chem. Soc., Dalton Trans.* **2000**, 727. (b) Tokunoh, R.; Sodeoka, M.; Aoe, K.; Shibasaki, M. *Tetrahedron Lett.* **1995**, *36*, 8038. (c) Melanson, R.; Rochon, F. D. *Can. J. Chem.* **1975**, *53*, 2371. (d) Svinning, T.; Mo, F.; Bruun, T. *Acta Crystallogr., Sect. B* **1976**, *32*, 759. (e) Helena, R.; Francisco, P.; Teresa, M.; Gambardella, P.; Rodrigues, A. M. G. D.; Souza, G. F.; Filgueiras, C. A. L. *Acta Crystallogr., Sect. C* **1995**, *51*, 604. (f) Selvaraju, R.; Panchanatheswaran, K.; Thiruvalluvar, A.; Parthasarathi, V. *Acta Crystallogr., Sect. C* **1995**, *51*, 606.
- (8) (a) Bu, X.-H.; Chen, W.; Lu, S.-L.; Zhang, R.-H.; Liao, D.-Z.; Shionoya, M.; Brisse, F.; Ribas, J. *Angew. Chem., Int. Ed.* **2001**, *40*, 3201. (b) Bu, X.-H.; Chen, W.; Du, M.; Zhang, R.-H. *CrystEngComm* **2001**, *3*, 131. (c) Bu, X.-H.; Weng, W.; Li, J.-R.; Chen, W.; Zhang, R.-H. *Inorg. Chem.* **2002**, *41*, 413. (d) Bu, X.-H.; Weng, W.; Du, M.; Chen, W.; Li, J.-R.; Zhang, R.-H.; Zhao, L.-J. *Inorg. Chem.* **2002**, *41*, 1007. (e) Li, J.-R.; Zhang, R.-H.; Bu, X.-H.; Chen J.-T. *J. Rare Earths* **2002**, *20*, 359. (f) Zhang, R.-H.; Ma, B.-Q.; Bu, X.-H.; Wang H.-G.; Yao, X.-K. *Polyhedron* **1997**, *16*, 1123 and 1787. (g) Li, J.-R.; Du, M.; Bu, X.-H.; Zhang, R.-H. *J. Solid State Chem.* **2003**, *173*, 20. (9) (a) Zhu, F.-C.; Shao, P.-X.; Yao, X.-K.; Wang, H.-G. *Inorg. Chim. Acta* **1990**, *171*, 85. (b) Bao, J.-C.; Shao, P.-X.; Wang, R.-J.; Wang, H.-G.; Yao, X.-K. *Polyhedron* **1995**, *14*, 927.

{[Eu(μ -*meso*-L)(*rac*-L)₂(CH₃OH)₂](ClO₄)₃]_n (**3**). Yield: 60%. Anal. Calcd for C₂₀H₅₀Cl₃O₂₀S₆Eu (%): C, 22.63; H, 4.75. Found: C, 22.22; H, 4.19. IR (KBr pellet, cm⁻¹): 3396s, 1636m, 1457w, 1417w, 1145s, 1115s, 1088s, 1003s, 779w, 693w, 637m, 627s. Decomposition temperature: 190 °C.

{[Gd(μ -*meso*-L)(*rac*-L)₂(CH₃OH)₂](ClO₄)₃]_n (**4**). Yield: 56%. Anal. Calcd for C₂₀H₅₀Cl₃O₂₀S₆Gd (%): C, 22.52; H, 4.73. Found: C, 22.21; H, 4.23. IR (KBr pellet, cm⁻¹): 3406s, 1637m, 1457w, 1409w, 1146s, 1116s, 1087s, 1003s, 779w, 683w, 637m, 626m. Decomposition temperature: 200 °C.

{[Tb(μ -*meso*-L)(*rac*-L)₂(CH₃OH)₂](ClO₄)₃]_n (**5**). Yield: 61%. Anal. Calcd for C₂₀H₅₀Cl₃O₂₀S₆Tb (%): C, 22.49; H, 4.72. Found: C, 22.76; H, 4.28. IR (KBr pellet, cm⁻¹): 3386s, 1636m, 1458w, 1418w, 1146s, 1115s, 1088s, 1002s, 778w, 682w, 637m, 627s. Decomposition temperature: 220 °C.

{[Dy(μ -*meso*-L)(*rac*-L)₂(CH₃OH)₂](ClO₄)₃]_n (**6**). Yield: 53%. Anal. Calcd for C₂₀H₅₀Cl₃O₂₀S₆Dy (%): C, 22.41; H, 4.70. Found: C, 22.18; H, 4.29. IR (KBr pellet, cm⁻¹): 3384s, 1635m, 1458w, 1418w, 1146s, 1115s, 1089s, 1003s, 796w, 682m, 637m, 627s. Decomposition temperature: 215 °C.

{[Yb(μ -*meso*-L)(*rac*-L)₂(CH₃OH)₂](ClO₄)₃]_n (**7**). Yield: 57%. Anal. Calcd for C₂₀H₅₀Cl₃O₂₀S₆Yb (%): C, 22.19; H, 4.66. Found: C, 21.60; H, 4.31. IR (KBr pellet, cm⁻¹): 3417s, 1646m, 1457w, 1412w, 1146s, 1116s, 1087s, 1004s, 778w, 693w, 637m, 627s. Decomposition temperature: 194 °C.

Synthesis of [Yb(μ -*meso*-L)_{1.5}(NO₃)₃]_n (8**).** Yb(NO₃)₃·*n*H₂O (0.2 mmol) in anhydrous MeOH (4 mL) was dehydrated by adding triethylorthoformate (3 mL) for ca. 30 min. An anhydrous CHCl₃ solution (4 mL) of *meso*-L (0.4 mmol) was added dropwise to the above mixture, which was further stirred at 60–70 °C for 1 h, then cooled to room temperature. After the filtration, the filtrate was left to stand at room temperature. Colorless single crystals were obtained after several days by slow evaporation of the solvent. Yield: 45%. Anal. Calcd for C₉H₂₁N₃O₁₂S₃Yb (%): C, 17.09; H, 3.35. Found: C, 16.75; H, 3.07. IR (KBr pellet, cm⁻¹): 2988w, 2943w, 1494s, 1384s, 1303s, 1023s, 988s, 815m, 747m. Decomposition temperature: 267 °C.

Synthesis of [La(μ -*meso*-L)_{2.5}(NCS)₃]_n (9**).** Colorless single crystals of **9** were obtained by the same procedure as for **8** but using Ln(NCS)₃·*n*H₂O instead of Ln(NO₃)₃·*n*H₂O. Yield: 43%. Anal. Calcd for C₁₈H₃₅N₃O₅S₈La (%): C, 28.12; H, 4.59. Found: C, 27.35; H, 4.12. IR (KBr pellet, cm⁻¹): 2978w, 2918w, 2057s, 1618w, 1452m, 1384s, 1001s, 825w, 627w. Decomposition temperature: 231 °C.

X-ray Diffraction Measurements. Single-crystal X-ray diffraction measurements of *meso*-L and all the complexes were carried out on a Bruker Smart 1000 CCD diffractometer with graphite-monochromatized Mo K α radiation ($\lambda = 0.71073$ Å) at 293 K. Empirical absorption corrections were applied using the SADABS program.^{11a} All structures were solved by direct methods, and refined by full-matrix least-squares methods on F^2 using the SHELXTL program package.^{11b} Anisotropic displacement parameters were refined for all non-hydrogen atoms. No attempt was made to locate the hydrogen of MeOH in **1–7**. The other hydrogen atoms were included in calculated positions and refined with isotropic thermal parameters riding on the parent atoms. The rotational disorder of ClO₄⁻ observed in the complexes was modeled as partially occupied tetrahedral rigid bodies pivoting about Cl.

Moreover, in the structures except for **4**, one of the three sulfur atoms in each crystallographic asymmetry unit is positional disorder and the statistical occupancy factors of S2 (the other disordered one marks S2') are 66 in **1**, 74 in **2**, 90 in **3**, 90 in **5**, 70 in **6**, and 60% in **7**. In **8** and **9** the positional disorders of one of the sulfur atoms in their asymmetry unit were also observed and the occupancy was distributed statistically, respectively. The summary of the crystallographic data and the details for structural refinement are given in Table 1.

Results and Discussion

Characterization and Structure of *meso*-L. The melting point (141–143 °C) of *meso*-L is higher than that of *rac*-L (124–126 °C), being in agreement with other disulfoxide enantiomers.¹² The IR data of *meso*-L show the characteristic bands of the sulfinyl group (S=O) at 1018 cm⁻¹, and a C–S stretch vibration at 770 cm⁻¹.¹³ An ORTEP view of the *meso*-L is given in Figure 1, and the selected bond distances and angles are listed in Table 2. The structure of *meso*-L has the *S,R* configuration with an inversion center at the midpoint of the central C–C bond. The torsion angles of O(1)–S(1)–C(2)–C(1) and C(2)–S(1)–C(3)–C(3A) are –65.5(3) and 175.4(3)°, respectively, and the S–O vectors are parallel and point to the opposite directions. These cases are similar to those in *meso*-1,2-bis(methylsulfinyl)ethane^{7d} and *meso*-1,2-bis(phenylsulfinyl)ethane.¹² The average S–O bond distance [1.509(2) Å] and bond angles of C–S–C [96.1(1)°] and O–S–C [106.8(1)°] are also nearly in agreement with the values reported for free sulfoxide and disulfoxides.^{7d,12}

Synthesis and General Characterization of **1–9.** The reactions of *meso*-L with Ln(ClO₄)₃ [or Ln(NO₃)₃, Ln(NCS)₃] in MeOH/triethylorthoformate/CHCl₃ gave the complexes {[Ln(μ -*meso*-L)(*rac*-L)₂(CH₃OH)₂](ClO₄)₃]_n, [Yb(μ -*meso*-L)_{1.5}(NO₃)₃]_n, and [La(μ -*meso*-L)_{2.5}(NCS)₃]_n. The results of elemental analyses for all the complexes were in good agreement with the theoretical requirements of their compositions. To investigate the influences of the metal/ligand ratio on the structures of complexes we prepared **1** and **7** in a 1:2 metal/ligand ratio, and **8** and **9** in a 1:3 ratio; the complexes obtained under these conditions have the same compositions as those described above, and this indicates that the structures of these complexes are not very sensitive to the metal/ligand ratio. The complexes are stable in air, and **1–7** decompose at about 200 °C, **8** decomposes at 267 °C, and **9** decomposes at 231 °C. In the IR spectra of **1–9**, the absorption bands of S=O stretching vibrations at ~1000 cm⁻¹ (988 cm⁻¹ for **8**) are lower than the corresponding S=O vibration in the free ligand (1018 cm⁻¹), indicating that the ligands are bound to Ln^{III} through the sulfinyl oxygen atoms.¹³ The existence of ClO₄⁻, NO₃⁻, and NCS⁻ anions in the complexes was also confirmed by IR spectra.

Crystal Structures of **1–7.** These seven complexes are isostructural and consist of cation chains of [Ln(μ -*meso*-L)-

(11) (a) Sheldrick, G. M. *SADABS, Siemens Area Detektor Absorption Correction Program*; University of Gottingen: Gottingen, Germany, 1994. (b) Sheldrick, G. M. *SHELXL-97, program for X-ray Crystal Structure Refinement*; University of Gottingen: Gottingen, Germany, 1997.

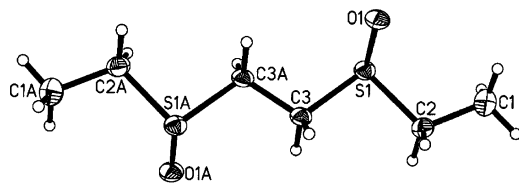
(12) (a) Cattalini, L.; Michelon, G.; Marangoni, G.; Pelizzi, G. *J. Chem. Soc., Dalton Trans.* **1979**, 296. (b) Ternay, A. L., Jr.; Lin, J.; Sutliff, T.; Chu, S. S. C.; Chung, B. *J. Org. Chem.* **1978**, *43*, 15.
(13) (a) Kagan, H. B.; Ronan, B. *Rev. Heteroat. Chem.* **1992**, *7*, 92. (b) Davies, J. A. *Adv. Inorg. Chem. Radiochem.* **1981**, *24*, 115.

Table 1. Crystallographic Data and Structural Refinement for *meso-L* and the Complexes 1–9

	<i>meso-L</i>	1	2	3	4
formula	C ₆ H ₁₄ O ₂ S ₂	C ₂₀ H ₅₀ Cl ₃ O ₂₀ S ₆ La	C ₂₀ H ₅₀ Cl ₃ O ₂₀ S ₆ Nd	C ₂₀ H ₅₀ Cl ₃ O ₂₀ S ₆ Eu	C ₂₀ H ₅₀ Cl ₃ O ₂₀ S ₆ Gd
<i>M_r</i>	182.29	1048.22	1053.55	1061.27	1066.56
space group	<i>P</i> $\bar{1}$	<i>C2/c</i>	<i>C2/c</i>	<i>C2/c</i>	<i>C2/c</i>
temp (K)	293(2)	293(2)	293(2)	293(2)	293(2)
<i>a</i> (Å)	5.363(3)	20.380(6)	20.109(6)	19.964(8)	20.107(6)
<i>b</i> (Å)	5.616(3)	11.787(3)	11.516(4)	11.533(4)	11.469(4)
<i>c</i> (Å)	8.773(6)	19.898(5)	19.466(6)	19.291(7)	19.347(6)
α (deg)	89.078(10)	90	90	90	90
β (deg)	84.380(10)	105.819(7)	105.896(5)	105.919(6)	105.707(5)
γ (deg)	64.981(9)	90	90	90	90
<i>V</i> (Å ³)	238.2(2)	4599(21)	4336(2)	4271(3)	4295(2)
<i>D_c</i> (Mg/m ³)	1.271	1.514	1.614	1.650	1.649
<i>Z</i>	2	4	4	4	4
μ (mm ⁻¹)	0.507	1.438	1.738	2.017	2.090
<i>R</i> ₁ ^a [<i>I</i> = 2 σ (<i>I</i>)]	0.0413	0.0451	0.0312	0.0557	0.0391
<i>wR</i> ₂ ^b (all data)	0.1086	0.1077	0.0793	0.1061	0.1021

	5	6	7	8	9
formula	C ₂₀ H ₅₀ Cl ₃ O ₂₀ S ₆ Tb	C ₂₀ H ₅₀ Cl ₃ O ₂₀ S ₆ Dy	C ₂₀ H ₅₀ Cl ₃ O ₂₀ S ₆ Yb	C ₉ H ₂₁ N ₃ O ₁₂ S ₃ Yb	C ₁₈ H ₃₅ N ₃ O ₅ S ₈ La
<i>M_r</i>	1068.23	1071.80	1082.35	632.51	768.88
space group	<i>C2/c</i>	<i>C2/c</i>	<i>C2/c</i>	<i>P</i> $\bar{1}$	<i>P</i> $\bar{1}$
temp (K)	293(2)	293(2)	293(2)	293(2)	293(2)
<i>a</i> (Å)	19.976(8)	20.001(6)	20.015(4)	9.524(4)	9.32(1)
<i>b</i> (Å)	11.584(5)	11.481(4)	11.379(7)	10.176(4)	13.11(2)
<i>c</i> (Å)	19.242(8)	19.222(6)	19.017(1)	12.987(5)	16.21(2)
α (deg)	90	90	90	92.607(7)	98.21(2)
β (deg)	105.831(7)	105.656(5)	105.750(5)	91.870(7)	105.02(2)
γ (deg)	90	90	90	117.236(6)	104.12(2)
<i>V</i> (Å ³)	4284(3)	4250(2)	4169(2)	1116.0(8)	1811(4)
<i>D_c</i> (Mg/m ³)	1.656	1.675	1.724	1.882	1.410
<i>Z</i>	4	4	4	2	2
μ (mm ⁻¹)	2.198	2.309	2.805	4.527	1.669
<i>R</i> ₁ ^a [<i>I</i> = 2 σ (<i>I</i>)]	0.0471	0.0381	0.0269	0.0346	0.1014
<i>wR</i> ₂ ^b (all data)	0.1144	0.0784	0.0690	0.0975	0.2366

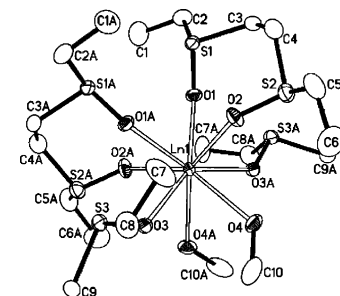
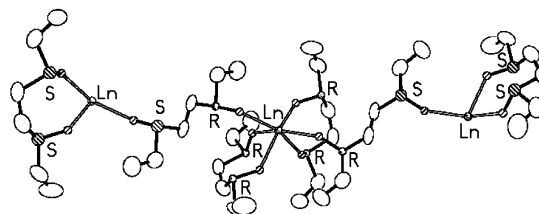
$$^a R_1 = \sum ||F_o| - |F_c|| / \sum |F_o|. \quad ^b wR_2 = \{ \sum [w(F_o^2 - F_c^2)^2] / \sum w(F_o^2)^2 \}^{1/2}.$$

**Figure 1.** ORTEP view of the ligand *meso-L* with 30% thermal ellipsoid probability.**Table 2.** Selected Bond Distances (Å), Angles (deg), and Torsion Angles (deg) for *meso-L*

S(1)–O(1)	1.509(2)	O(1)–S(1)–C(2)	107.1(1)
S(1)–C(2)	1.816(3)	O(1)–S(1)–C(3)	106.6(1)
S(1)–C(3)	1.824(3)	C(2)–S(1)–C(3)	96.1(1)
O(1)–S(1)–C(3)–C(3A) ^a	65.5(3)	O(1)–S(1)–C(2)–C(1)	–65.9(3)
C(2)–S(1)–C(3)–C(3A)	175.4(3)	C(3)–S(1)–C(2)–C(1)	–175.3(2)

^a Symmetry code: A $-x + 1, -y + 1, -z$.

(*rac-L*)₂(CH₃OH)₂]³⁺ and ClO₄[–]. The environment around Ln^{III} is shown in Figure 2, and a segment of cationic chain is shown in Figure 3. Each Ln^{III} has an octacoordinated distorted square antiprism environment formed by eight oxygen atoms in which six are from four distinct *L* ligands and two are from MeOH. Two *L* ligands are chelated to a Ln^{III} to form seven-membered coordination rings, and the other two *L* ligands act as bis-monodentate bridge to link adjacent Ln^{III} ions to form an undulate chain. To our knowledge, these are first examples for disulfoxide complexes in which chelating and bridging coordination modes

**Figure 2.** ORTEP view of the mononuclear unit in 1–7 showing the coordination environment of the Ln^{III} center.**Figure 3.** Perspective view of the chain segment showing the steric features (*S* or *R*) of *L* in 1–7. Coordinated MeOH molecules and H atoms were omitted for clarity.

of ligands coexist in the same molecule. The two adjacent bridging *L* ligands form a “V-joint” at the Ln^{III} center, which causes the chain undulation with an Ln^{III}⋯Ln^{III}⋯Ln^{III} angle of 148.9 for 1, 148.4 for 2, 147.5 for 3, 148.2 for 4, 146.9 for 5, 147.4 for 6, and 147.1° for 7, and the shortest intramo-

Table 3. Selected Bond Distances (Å) and Angles (deg) for **1–7**

	1	2	3	4	5	6	7
Ln(1)–O(1)	2.527(6)	2.433(3)	2.392(4)	2.383(4)	2.379(4)	2.363(3)	2.309(4)
Ln(1)–O(2)	2.468(7)	2.386(3)	2.344(4)	2.347(4)	2.328(4)	2.316(3)	2.267(5)
Ln(1)–O(3)	2.493(6)	2.403(2)	2.362(4)	2.357(4)	2.351(4)	2.336(3)	2.270(5)
Ln(1)–O(4)	2.635(6)	2.538(3)	2.475(4)	2.489(4)	2.453(4)	2.452(3)	2.428(5)
S(1)–O(1)	1.536(5)	1.515(3)	1.506(4)	1.525(4)	1.506(4)	1.508(3)	1.517(4)
S(2)–O(2)	1.550(5)	1.529(3)	1.528(4)	1.512(4)	1.522(5)	1.517(4)	1.516(4)
S(3)–O(3)	1.549(5)	1.527(3)	1.522(4)	1.528(4)	1.520(4)	1.519(3)	1.517(4)
O(1)–Ln(1)–O(2)	71.7(2)	73.1(1)	73.7(2)	74.1(2)	74.0(2)	74.4(1)	75.3(1)
O(1)–Ln(1)–O(3)	147.5(1)	148.39(9)	149.1(1)	148.9(1)	149.6(1)	149.3(1)	149.5(1)
O(1)–Ln(1)–O(4)	131.6(2)	131.67(9)	131.4(1)	131.9(2)	131.6(1)	131.5(1)	131.9(1)
O(2)–Ln(1)–O(3)	104.3(2)	104.4(1)	103.8(2)	104.1(2)	103.9(2)	103.7(1)	103.6(1)
O(2)–Ln(1)–O(4)	74.4(2)	73.9(1)	73.6(2)	73.7(2)	73.6(2)	73.5(1)	73.4(2)
O(3)–Ln(1)–O(4)	74.1(2)	74.23(9)	74.1(1)	74.2(2)	73.7(1)	74.1(1)	74.1(1)
S(1)–O(1)–Ln(1)	136.6(2)	135.4(2)	135.3(2)	134.5(2)	134.8(2)	134.8(2)	134.4(2)
S(2)–O(2)–Ln(1)	134.0(3)	133.5(2)	132.6(3)	133.1(3)	132.5(3)	132.5(2)	132.3(2)
S(3)–O(3)–Ln(1)	136.3(2)	136.0(2)	135.9(2)	135.7(2)	135.7(2)	135.6(2)	135.5(2)

Table 4. Selected Torsion Angles (deg) for the Chelating and the Bridging **L** Found in **1–7**

compd	Ln(1)–O(1)–S(1)–C(2)	Ln(1)–O(1)–S(1)–C(3)	Ln(1)–O(2)–S(2)–C(4)	Ln(1)–O(2)–S(2)–C(5)
1	–164.9(3)	92.1(4)	107.4(4)	–149.6(4)
2	–164.5(2)	92.5(3)	107.7(4)	–149.6(3)
3	–164.2(4)	92.4(4)	107.1(4)	–149.7(4)
4	–164.6(4)	92.8(4)	107.1(5)	–148.6(4)
5	–164.2(4)	92.4(4)	107.8(4)	–148.6(4)
6	–165.0(4)	92.2(3)	108.0(3)	–149.6(4)
7	–165.0(3)	91.7(3)	108.0(3)	–149.4(3)

compd	Ln(1)–O(3)–S(3)–C(8)	Ln(1)–O(3)–S(3)–C(9)	O(1)–S(1)···S(2)–O(2) ^a	O(3)–S(3)···S(3A)–O(3A) ^b
1	–101.6(4)	156.4(3)	–56.7(5)	180
2	–100.2(3)	158.1(2)	–57.4(3)	180
3	–99.2(4)	158.8(3)	–57.7(6)	180
4	–99.4(5)	158.3(3)	–57.6(4)	180
5	–99.0(4)	159.0(3)	–58.0(5)	180
6	–99.1(3)	159.2(3)	–57.9(4)	180
7	–98.8(3)	159.6(2)	–57.7(3)	180

^a In chelating **L**. ^b In bridging **L**. Symmetry code: A $-x + 1, -y + 1, -z + 1$.

lecular Ln···Ln distance is 10.326, 10.115, 10.047, 10.059, 10.038, 10.014, and 9.914 Å for **1–7**, respectively.

As shown in Table 3, four pairs of Ln–O bond lengths around each Ln^{III} are different with one relatively shorter and one longer in each chelating ligand, and the Ln–O bond length of the bridging ligands lies between the two Ln–O bond lengths of the chelating ligands. The oxygen atoms of MeOH form the longest Ln–O bond in the complexes. As expected, the Ln–O bond lengths shorten gradually from the early lanthanide to the late lanthanide due to lanthanide contraction. In addition, the O···O distances in the chelating (2.926–2.795 Å) and bridging (5.726–5.662 Å) ligands are obviously different, showing the structural flexibility of the disulfoxide ligand.

In all cases, the sulfinyl groups retain their double bond character, but undergo some changes when coordinating to Ln^{III} ions, namely, the average S=O bond distance [1.522(7) Å] is a little longer than that in the free disulfoxide [1.509(2) Å]. The S=O bond lengths are shortening gradually with the decreasing of the atom radius of lanthanide. This may be attributed to the enhancement of stereo repulsion among ligands in the complexes. In addition, the M–O–S angles (~134°) for the chelating and bridging ligands are larger than those of other sulfoxide transition metal complexes.^{4c}

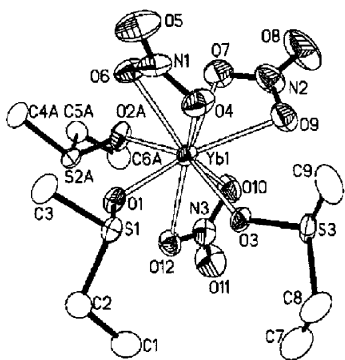
It is noteworthy that the **L** ligands take three different configurations in the complexes: (a) the *meso* form, acting as bridges with an alternative arrangement of *R,S* and *S,R* orders for the configuration of sulfur atoms in the single μ -chains; (b) the *rac* form, adopting *R,R* or *S,S* configuration to chelate Ln^{III} atoms. The sulfur atoms bound to the oxygen atoms around the same Ln^{III} center adopt a stereoisomeric form, *R* or *S*, and a group of the sulfur atoms of *S* configuration and other *R* configuration arrange alternatively in the chains (Figure 3), so the chains as a whole are nonchiral. It is rare that three kinds of isomers occur simultaneously in the same complex, and to our knowledge, this is also the first example in the disulfoxide complexes. In addition, when *meso-L* reacts with Ln(ClO₄)₃ the resulting complexes contain not only the *meso* (*R,S*) but the *rac* (*S,S* or *R,R*) isomers of the ligands, indicating the configuration changes of **L** during the complex formation process.

The sulfoxide ligands through oxygen coordination can be stereochemically classified into *trans* and *cis* arrangements.^{12a} According to the torsion angles M–O–S–C of the complexes, the ligands **L** are *trans-trans* arranged in all the complexes (Table 4), and the average pseudo-torsion angles of O=S···S=O are different in chelating ligands (the whole average value, –57.6°) and bridging ligands (180°) in **1–7**.

Table 5. Selected Bond Distances (Å), Angles (deg), and Torsion Angles (deg) for **8**

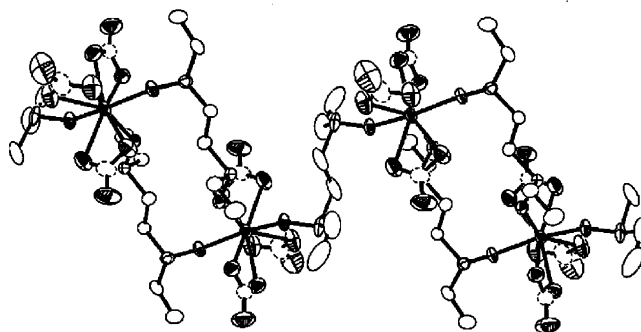
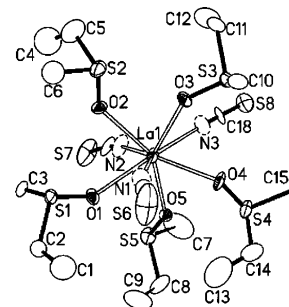
Yb(1)–O(1)	2.283(4)	Yb(1)–O(7)	2.380(6)
Yb(1)–O(2A) ^a	2.261(4)	Yb(1)–O(9)	2.461(5)
Yb(1)–O(3)	2.256(4)	Yb(1)–O(10)	2.389(5)
Yb(1)–O(4)	2.425(5)	Yb(1)–O(12)	2.454(5)
Yb(1)–O(6)	2.484(5)		
O(1)–Yb(1)–O(2A)	84.7(2)	O(4)–Yb(1)–O(9)	76.5(2)
O(1)–Yb(1)–O(3)	79.7(2)	O(4)–Yb(1)–O(10)	147.3(2)
O(1)–Yb(1)–O(4)	79.0(2)	O(4)–Yb(1)–O(12)	145.9(2)
O(1)–Yb(1)–O(6)	76.3(2)	O(6)–Yb(1)–O(2A)	71.6(2)
O(1)–Yb(1)–O(7)	147.9(2)	O(6)–Yb(1)–O(7)	73.1(2)
O(1)–Yb(1)–O(9)	147.9(2)	O(6)–Yb(1)–O(9)	103.5(2)
O(1)–Yb(1)–O(10)	127.3(2)	O(6)–Yb(1)–O(10)	143.5(2)
O(1)–Yb(1)–O(12)	75.0(2)	O(6)–Yb(1)–O(12)	138.3(2)
O(3)–Yb(1)–O(2A)	152.1(2)	O(7)–Yb(1)–O(2A)	76.6(2)
O(3)–Yb(1)–O(4)	76.3(2)	O(7)–Yb(1)–O(9)	52.2(2)
O(3)–Yb(1)–O(6)	125.7(2)	O(7)–Yb(1)–O(10)	76.2(2)
O(3)–Yb(1)–O(7)	126.9(2)	O(7)–Yb(1)–O(12)	123.8(2)
O(3)–Yb(1)–O(9)	74.6(2)	O(9)–Yb(1)–O(2A)	126.3(2)
O(3)–Yb(1)–O(10)	88.8(2)	O(9)–Yb(1)–O(10)	71.5(2)
O(3)–Yb(1)–O(12)	77.7(2)	O(9)–Yb(1)–O(12)	116.9(2)
O(4)–Yb(1)–O(2A)	123.2(2)	O(10)–Yb(1)–O(2A)	82.5(2)
O(4)–Yb(1)–O(6)	51.7(2)	O(10)–Yb(1)–O(12)	52.3(2)
O(4)–Yb(1)–O(7)	89.6(2)	O(12)–Yb(1)–O(2A)	76.1(2)
Yb(1)–O(1)–S(1)–C(2)	–130.6(3)	Yb(1)–O(3)–S(3)–C(8)	–162.1(6)
Yb(1)–O(1)–S(1)–C(3)	124.5(4)	Yb(1)–O(3)–S(3)–C(8)	92.2(5)
Yb(1A)–O(2)–S(2)–C(4)	–110.0(5)	O(1)–S(1)···S(2)–O(2)	67.8(3)
Yb(1A)–O(2)–S(2)–C(5)	148.3(5)	O(3)–S(3)···S(3B)–O(3B)	180

^a Symmetry codes: A $-x + 1, -y, -z$; B $-x + 1, -y, -z + 1$.

**Figure 4.** ORTEP view of the mononuclear segment of **8** showing the coordination environments of the Yb^{III} center.

In order to investigate the influences of counteranions on the framework formation of complexes, Ln(NO₃)₃ and Ln(SCN)₃ were used instead of Ln(ClO₄)₃ to react with *meso-L* under similar conditions, and two complexes [Yb(μ -*meso-L*)_{1.5}(NO₃)₃]_n (**8**) and [La(μ -*meso-L*)_{2.5}(NCS)₃]_n (**9**) were obtained.

Crystal Structure of 8. The structure of **8** contains a neutral single–double bridging chain in which the Yb^{III} ion is 9-coordinated to three oxygen atoms of three *meso-L* ligands and six oxygen atoms of three bidentate nitrate ions in a distorted tricapped trigonal prism geometry (Figure 4). As shown in Table 5 the Yb–O distances fall into two distinct groups with those to the *meso-L* oxygen atoms being in the range of 2.256(4)–2.283(4) Å and those to the nitrate groups in the range of 2.380(6)–2.484(5) Å. The bond angles around Yb^{III} ion range from 51.7(2) to 89.6(2)°. In **8** two Yb^{III} centers are bridged by two *meso-L* to give a 14-membered macrometallacycle. Further, these macrometallacyclic units are linked by other ligands to form a single–double

**Figure 5.** Perspective view of the single–double chain in **8**.**Figure 6.** ORTEP view of the mononuclear segment of **9** showing the coordination environments of the La^{III} center.

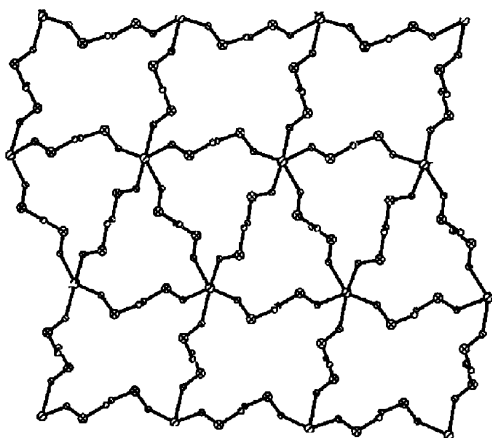
bridging chain (Figure 5). The Yb···Yb distances in the ring and in the single bridging units are 8.180 and 8.869 Å, respectively. All the *meso-L* ligands act as bridges to link Yb^{III} centers in bis-monodentate coordination mode, and present *R,S* configuration as that in free ligand and *trans-trans* arrangement formation (see the torsion angles of M–O–S–C in Table 5). However, the conformations of the ligands in double and single bridging units are different. Those ligands acting as single bridges have an O=S···S=O quasi-torsion angle of 180°, but that value in the double bridging ligands is 67.8(3)°.

Crystal Structure of 9. Complex **9** has a 2-D framework structure as in the analogous complexes [Ln(μ -*meso-L'*)_{2.5}(NCS)₃]_n (Ln = Nd or Yb, L' = 1,2-bis(propylsulfinyl)ethane).^{8c} Each La^{III} ion is coordinated by five oxygen atoms from five distinct *meso-L* and three nitrogen atoms of three SCN[–] anions to form a distorted square antiprism geometry (Figure 6). As shown in Table 6, five La–O distances are nearly equivalent and falling into a narrow range of 2.50(1)–2.55(1) Å, and the La–N distances are in the range of 2.57(2)–2.67(2) Å. The bond angles around the La^{III} center range from 71.2(3) to 85.5(4)°. The S–O distances and C–S–C angles are within expected ranges. In **9**, each La^{III} center is linked to five other La^{III} centers by the L bridges to form a 5-connected 2-D (3/4,5) network containing two types of macrometallacyclic arrays (Figure 7). One type is a 28-membered ring with quadrilateral grid formed by four metal centers and four L ligands, and the other one is a 21-membered triangle ring made up of three metal centers and three L ligands. The distances of La···La in the 28-membered ring are 9.321(2) and 9.551(3) Å, and those in the 21-membered ring are 9.321(2), 9.662(3), and 9.979(2) Å,

Table 6. Selected Bond Distances (Å), Angles (deg), and Torsion Angles (deg) for **9**

La(1)–O(1)	2.54(1)	La(1)–O(5A) ^a	2.50(1)
La(1)–O(2)	2.55(1)	La(1)–N(1)	2.67(2)
La(1)–O(3)	2.51(1)	La(1)–N(2)	2.57(2)
La(1)–O(4)	2.55(1)	La(1)–N(3)	2.66(2)
O(1)–La(1)–O(2)	76.2(3)	N(2)–La(1)–O(2)	77.5(4)
O(1)–La(1)–O(3)	140.6(4)	N(2)–La(1)–O(3)	122.7(5)
O(1)–La(1)–O(4)	123.0(4)	N(2)–La(1)–O(4)	136.9(4)
O(2)–La(1)–O(3)	72.5(3)	N(3)–La(1)–O(1)	141.7(4)
O(2)–La(1)–O(4)	142.2(3)	N(3)–La(1)–O(2)	111.9(5)
O(3)–La(1)–O(4)	74.1(4)	N(3)–La(1)–O(3)	73.8(4)
N(1)–La(1)–O(1)	74.2(4)	N(3)–La(1)–O(4)	74.4(5)
N(1)–La(1)–O(2)	81.4(5)	N(1)–La(1)–N(2)	143.1(5)
N(1)–La(1)–O(3)	77.9(5)	N(1)–La(1)–N(3)	142.7(5)
N(1)–La(1)–O(4)	74.8(5)	N(2)–La(1)–N(3)	73.9(5)
N(2)–La(1)–O(1)	71.6(5)		
C(2)–S(1)–O(1)–La(1)	–141(1)	C(11)–S(3)–O(3)–La(1)	139(1)
C(3)–S(1)–O(1)–La(1)	116(1)	C(14)–S(4)–O(4)–La(1)	–118(1)
C(5)–S(2)–O(2)–La(1)	137(1)	C(15)–S(4)–O(4)–La(1)	139(1)
C(6)–S(2)–O(2)–La(1)	–129(1)	O(2)–S(2)···S(5)–O(5)	151(1)
C(10)–S(3)–O(3)–La(1)	–118(1)		

^a Symmetry code: $A x + 1, y, z$.

**Figure 7.** Perspective view of the 2-D network in **9** with SCN[–] omitted for clarity.

respectively. In the complex all the ligands present bis-monodentate coordination mode and *trans-trans* arrangement form, and adopt the same *R,S* configuration as that in the free ligand (*meso-L*).

Some 1-D and 2-D lanthanide coordination polymers with 1,2-bis(propylsulfinyl)ethane (**L'**) and 1,4-bis(phenylsulfinyl)butane (**L''**) have been reported in our previous work,^{8c,e,f} and the structure of complex **9** reported in this work is similar to that of [Ln(μ -*meso-L'*)_{2.5}(NCS)₃]_n.^{8c} The structures of these complexes^{8c,e,f} were found to be sensitive to the factors such as counteranions, metal ions, and solvents. But configuration change of ligands has not been observed in these reported complexes. The observed configuration change of disulfoxide ligands of the complexes reported in this work is the first example for the complexes with disulfoxide ligands.

Photoluminescence of 3 and 5. The luminescent properties of lanthanide complexes, particularly those of Eu^{III} and Tb^{III}, can give useful information regarding their structures in solution and the solid state.¹⁴ The luminescent properties

Table 7. Absorption and Emission Spectra of **3** and **5**^a

compd	absorption ($\lambda_{\text{abs}}/\text{nm}$)	emission [excitation] ($\lambda_{\text{em}}/\text{nm}$)
3	206, 291, 362, 384, 394	(589, 592), 612, 658, 699 [394]
5	226, 240, 284, 350, 368, 378	(487, 491), (544, 549), (583, 589), 618 [368]

^a Also see Supporting Information.

of **3** and **5** in solid state were studied, and the results are summarized in Table 7. The excitation spectra of **3** [Eu^{III} (⁵D₀), λ_{em} in 200–600 nm region] and **5** [Tb^{III} (⁵D₄), λ_{em} in 200–500 nm region] show the absorption of the ligand and Ln^{III} ions, in which the absorption of the ligand is shown at 291 nm for **3** and 284 nm for **5**, respectively. Excitation at 394 (for **3**) or 368 nm (for **5**) results in intense emission. The emission spectrum of **3** in the range of 500–710 nm shows that four emission bands are resolved corresponding to the transitions from the ⁵D₀ excited state to ⁷F_J ($J = 1-4$). The 3-fold degeneracy of the ⁷F₁ free-ion state is split obviously to two components. The split of the so-called hypersensitive ⁵D₀ → ⁷F₂ is not obvious, but the transition is the strongest in the four transitions with three times the strength of the transition of ⁵D₀ → ⁷F₁. The emission spectrum shows that Eu^{III} in **3** has the lower symmetric coordination environment¹⁵ closing to *D*₂ symmetry. It is consistent with the result of the structural analysis of the complex. The emission spectrum of **5** contains four bands corresponding to the transitions of ⁵D₄ → ⁷F_J ($J = 3-6$) in which each band is split obviously to two components. The intensity of the hypersensitive ⁵D₄ → ⁷F₅ transition is close to six times that of other bands. These results show that the complex has excellent single color property.

Summary

A series of lanthanide complexes of a disulfoxide ligand, *meso*-1,2-bis(ethylsulfinyl)ethane (*meso-L*), with different counteranions have been synthesized and characterized. All the complexes with Ln(ClO₄)₃ are isostructural, and consist of single μ -chains in which the 8-coordinated Ln^{III} are linked by **L**. The interesting features of these coordination polymers are as follows: (a) the binding of **L** to Ln^{III} presents two coordination modes, namely, bidentate chelating and bis-monodentate bridging; (b) three configurations of the ligand (*R,S*, *R,R*, and *S,S* forms) occur simultaneously in the same complex, and a coordination sphere with sulfur atoms of *R* configuration and an adjacent one with *S* configuration arrange alternatively in the chains; (c) when *meso-L* coordinates to Ln^{III}, the configuration change of partial ligands from *meso* to *rac* form was observed; (d) all the ligands (chelating and bridging) coordinated to Ln^{III} adopt a *trans-trans* arrangement. The complexes with Ln(NO₃)₃ and Ln(NCS)₃ have single–double chain and 5-connected 2-D (3/4,5) network structures, respectively, in which all the ligands show bis-monodentate bridging mode and *meso*

- (14) (a) Gajadhar-Plummer, A. S.; Ishenkumba, I. A.; White, A. J. P.; Williams, D. J. *Inorg. Chem.* **1999**, *38*, 1745. (b) Richardson, R. S. *Chem. Rev.* **1982**, *82*, 541. (c) Meares, C. F.; Wensel, T. G. *Acc. Chem. Res.* **1984**, *17*, 202.
 (15) Murray, G. M.; Sarrio, R. V.; Peterson, J. R. *Inorg. Chim. Acta* **1990**, *176*, 233.

configuration. The structural differences among **1–7**, **8**, and **9** show that counteranions play important roles in the framework formation of such coordination polymers.

Acknowledgment. The work was financially supported by the Outstanding Youth Foundation of NSFC (No. 20225101).

Supporting Information Available: The excitation and emission spectra of **3** and **5** (Figure S1–S4) and X-ray crystallographic file for *meso-L* and the complexes **1–9** (in CIF format). This material is available free of charge via the Internet at <http://pubs.acs.org>.

IC034772I